UCSF

UC San Francisco Previously Published Works

Title

Targeted Next-Generation Sequencing Reveals Divergent Clonal Evolution in Components of Composite Pleomorphic Xanthoastrocytoma-Ganglioglioma

Permalink

https://escholarship.org/uc/item/430411t5

Journal

Journal of Neuropathology & Experimental Neurology, 81(8)

ISSN

0022-3069

Authors

Lucas, Calixto-Hope G
Davidson, Christian J
Alashari, Mouied
et al.

Publication Date

2022-07-19

DOI

10.1093/jnen/nlac044

Peer reviewed

eScholarship.org Powered by the California Digital Library
University of California

J Neuropathol Exp Neurol
Vol. 81, No. 8, August 2022, pp. 650–657
doi: 10.1093/jnen/nlac044

OXFORD

ORIGINAL ARTICLE

Targeted Next-Generation Sequencing Reveals Divergent Clonal Evolution in Components of Composite Pleomorphic Xanthoastrocytoma-Ganglioglioma

Calixto-Hope G. Lucas, MD, Christian J. Davidson, MD, Mouied Alashari, MD, Angelica R. Putnam, MD, Nicholas S. Whipple, MD, Carol S. Bruggers, MD, Joe S. Mendez, MD, Samuel H. Cheshier, MD, PhD, Jeffrey B. Walker, MD, Biswarathan Ramani, MD, PhD, Cathryn R. Cadwell, MD, PhD, Daniel V. Sullivan, MD, Rufei Lu, MD, PhD, Kanish Mirchia, MD, Jessica Van Ziffle, PhD, Patrick Devine, MD, PhD, Ezequiel Goldschmidt, MD, PhD, Shawn L. Hervey-Jumper, MD, Nalin Gupta, MD, PhD, Nancy Ann Oberheim Bush, MD, PhD, David R. Raleigh, MD, PhD, Andrew Bollen, MD, Tarik Tihan, MD, Melike Pekmezci, MD, David A. Solomon, MD, PhD, Joanna J. Phillips, MD, PhD, and Arie Perry, MD

Abstract

Composite pleomorphic xanthoastrocytoma-ganglioglioma (PXA-GG) is an extremely rare central nervous system neoplasm with 2 distinct but intermingled components. Whether this tumor represents a "collision tumor" of separate neoplasms or a monoclonal neoplasm with divergent evolution is poorly understood. Clinicopathologic studies and capture-based next generation sequencing were performed on extracted DNA from all available PXA-GG at 2 medical centers. Five PXA-GG were diagnosed in 1 male and 4 female patients ranging from 13 to 25 years in age. Four arose within the cerebral hemispheres; 1 presented in the cerebellar vermis. DNA was sufficient for analysis in 4 PXA components and 3 GG components. Four paired PXA and GG components harbored *BRAF* p.V600E hotspot mutations. The 4 sequenced PXA components demonstrated *CDKN2A* homozygous deletion by sequencing with loss of p16 (protein product of *CDKN2A*) expression by immunohistochemistry, which was intact in all assessed GG components. The PXA components also demonstrated more frequent copy number alterations relative to paired GG components. In one PXA-GG, shared chromosomal copy number alterations were identified in both components. Our findings support divergent evolution of the PXA and GG components from a common *BRAF* p.V600E-mutant precursor lesion, with additional acquisition of *CDKN2A* homozygous deletion in the PXA component as is typically seen in conventional PXA.

Key Words: Collision tumor, Ganglioglioma, Intratumoral heterogeneity, Molecular neuropathology, Neurooncology, Pleomorphic xanthoastrocytoma, Precision medicine.

INTRODUCTION

Composite pleomorphic xanthoastrocytoma-ganglioglioma (PXA-GG) is an extremely rare neoplasm of

From the Department of Pathology, University of California, San Francisco, San Francisco, California, USA (C-HGL, BR, CRC, DVS, RL, KM, JVZ, PD, AB, TT, MP, DAS, JJP, AP); Department of Pathology, University of Utah, Salt Lake City, Utah, USA (CJD); Division of Pediatric Pathology, Department of Pathology, University of Utah, Salt Lake City, Utah, USA (MA, ARP); Division of Pediatric Hematology/Oncology, Department of Pediatrics, University of Utah, Salt Lake City, Utah, USA (NSW, CSB); Department of Neurosurgery, University of Utah/Huntsman Cancer Institute, Salt Lake City, Utah, USA (JSM); Division of Pediatric Neurosurgery, Department of Neurosurgery, Huntsman Cancer Institute, University of Utah, Intermountain Primary Children's Hospital, Salt Lake City, Utah, USA (SHC); Boise Pathology Group, St. Luke's, Boise, Idaho, USA (JBW); Clinical Cancer Genomics Laboratory, University of California, San Francisco, San Francisco, California, USA (JVZ, PD); Department of Neurological Surgery, University of California, San Francisco, San Francisco, California, USA (EG, SLH-J, NG, DRR, JJP, AP); Department of Pediatrics, University of California, San Francisco, San Francisco, USA (NG); Division of Neuro-Oncology, Department of Neurological Surgery, University of California, San Francisco, San Francisco, California, USA (NAOB); Department of Neurology, University of California, San Francisco, San Francisco, California, USA (NAOB); Department of Radiation Oncology, University of California, San Francisco, San Francisco, California, USA (DRR).

Send correspondence to: Arie Perry, MD, Department of Pathology, Division of Neuropathology, University of California, San Francisco, 505 Parnassus Avenue, Room M551, San Francisco, CA 94143; E-mail: arie.perry@ucsf.edu

C-HGL is supported by the UCSF Translational Brain Tumor Research Training Program, National Cancer Institute, National Institutes of Health (T32 CA151022) and the UCSF Brain Tumor SPORE Developmental Research Program, National Cancer Institute, National Institutes of Health (P50 CA097257). DAS is supported by the NIH Director's Early Independence Award from the Office of the Director, National Institutes of Health (DP5 OD021403).

The authors have no duality or conflicts of interest to declare.

Supplementary Data can be found at academic.oup.com/jnen.

© The Author(s) 2022. Published by Oxford University Press on behalf of American Association of Neuropathologists, Inc.
All rights reserved. For permissions, please email: journals.permissions@oup.com

the central nervous system that exhibits 2 distinct but intermingled components of both pleomorphic xanthoastrocytoma and ganglioglioma. To our knowledge, the first cases were reported by 2 different groups in 1992 (1, 2). Thirty years later, the current body of literature remains limited to small descriptive case series and single case reports due to the rarity or under recognition of this unique tumor type (3–13). These tumors tend to occur in the cerebral hemispheres of pediatric and young adult patients, although cases occurring in the cerebellum, in infants, and in older adults have also been reported. Clinically, patients often present with seizures and are found to have a superficial and well-demarcated lesion on neuroimaging. Resection is often curative, although malignant transformation of the PXA component can occur (7, 13).

While the molecular underpinnings of PXA and GG have been examined individually over the past few years (14–18), comprehensive genetic analysis of PXA-GG has not been performed to date. One case series (11) and a subsequent case report (12) demonstrated shared *BRAF* p.V600E mutation in paired PXA and GG components of PXA-GG but molecular analysis was limited to single-gene sequencing. Whether this tumor represents a "collision tumor" of clonally separate neoplasms or a monoclonal neoplasm with divergent evolution is poorly understood. Here, we report comprehensive clinicopathologic findings in 5 patients with composite GG-PXA, including molecular characterization of both the PXA and the GG components.

MATERIALS AND METHODS

Ethical Approval

This study was approved by the Committee on Human Research of the University of California, San Francisco, with a waiver of patient consent.

Patient Cohort and Tumor Samples

Five patients with PXA-GG were included in this study. Immunohistochemistry was performed on whole formalin-fixed, paraffin-embedded (FFPE) tissue sections. Staining was performed on a Leica Bond-III automated staining processor. Diaminobenzidine was used as the chromogen, followed by hematoxylin counterstain. Genomic DNA was extracted from FFPE tumor tissue using the QIAamp DNA FFPE Tissue Kit (Qiagen). Areas of homogenous PXA or GG components were identified on histology and macrodissected from either unstained slides or paraffin blocks, taking care to avoid contamination between the components.

Targeted Next-Generation Sequencing

Tumor tissue was selectively scraped from unstained slides or punched from FFPE blocks using biopsy punches (Integra Miltex Instruments, Princeton, NJ, Cat No. 33-31-P/25) to enrich for as high of tumor content as possible, as mentioned above. Genomic DNA was extracted from this macrodissected FFPE tumor tissue using the QIAamp DNA FFPE Tissue Kit (Qiagen, Germantown, MD). Targeted next-generation sequencing was performed using the UCSF500 Next-Generation Sequencing Panel as previously described (19, 20). Capture-based next-generation DNA sequencing was performed using an assay that targets all coding exons of 479 cancer-related genes, select introns and upstream regulatory regions of 47 genes to enable detection of structural variants including gene fusions, and DNA segments at regular intervals along each chromosome to enable genome-wide copy number and zygosity analysis, with a total sequencing footprint of 2.8 Mb (Supplementary Data Table S1). Multiplex library preparation was performed using the KAPA Hyper Prep Kit (Roche, Indianapolis, IN) according to the manufacturer's specifications using 250 ng of sample DNA. Hybrid capture of pooled libraries was performed using a custom oligonucleotide library (Nimblegen SeqCap EZ Choice). Captured libraries were sequenced as paired-end reads on an Illumina HiSeq 2500 instrument. Sequence reads were mapped to the reference human genome build GRCh37 (hg19) using the Burrows-Wheeler aligner. Recalibration and deduplication of reads were performed using the Genome Analysis Toolkit. Coverage and sequencing statistics were determined using Picard CalculateHsMetrics and Picard CollectInsertSizeMetrics. Single-nucleotide variant and small insertion/deletion mutation calling were performed with FreeBayes, Unified Genotyper, and Pindel. Large insertion/deletion and structural alteration calling were performed with Delly. Variant annotation was performed with Annovar. Single-nucleotide variants, insertions/deletions, and structural variants were visualized and verified using Integrative Genome Viewer. Genome-wide copy number and zygosity analysis were performed by CNVkit and visualized using NxClinical (Biodiscovery, El Segundo, CA).

RESULTS

PXA-GG Patient Cohort Characteristics

The 1 male and 4 female patients included in this series had a mean age of 18 years at time of initial diagnosis with a range of 13 to 25 years (Table 1). Imaging studies demonstrated contrast enhancement in all 5 cases, with 2 cases exhibiting intratumoral hemorrhage at presentation. Tumors appeared solid or mixed solid/cystic, overlapping with the appearance of conventional PXA and GG (Fig. 1). Tumors were located in temporal lobe (2), parietal lobe (1), frontal lobe (1), and posterior fossa (1). Presenting symptoms included new onset seizure in the 2 patients with temporal lobe tumors and headaches in the other 3 patients. Two patients underwent subtotal resection; patient #2 received post-operative radiotherapy with no evidence of recurrence at 22 months follow-up and patient #3 received post-operative radiotherapy followed by a MEK inhibitor with no evidence of recurrence at 27 months follow-up. Of the 3 patients that underwent gross total resection, 1 presented with recurrence at 18 months after initial surgery and underwent reresection. The other 2 received no adjuvant therapy and showed no evidence of disease recurrence. All patients are alive at time of last follow-up with a mean follow-up of 23 months (range 8–30 months).

TABLE 1. Clinical Data for the 5 Patients with "Composite Pleomorphic Xanthoastrocytoma-Ganglioglioma"

ID	Age at Initial Diagnosis	Sex	Clinical Presentation	Tumor Location	Preoperative Imaging Features	Histologic Diagnosis	EOR	Tumor Progression or Recurrence	Adjuvant Therapy	VS	Length of Follow-Up
#1	25 years	F	Seizure	Right temporal	Well-circumscribed, enhancing mass	Composite GG-PXA, grade 2	Gross total	No	None (surveillance only)	Alive	8 months
#2	18 years	F	Headaches, altered mental status	Cerebellar vermis	Hemorrhagic, enhancing mass	Composite GG-PXA, grade 2	Subtotal	No	Radiotherapy	Alive	22 months
#3	15 years	F	Headaches, speech impairment, hemiparesis	Right parietal	Hemorrhagic, enhancing mass	Composite GG-PXA, grade 3	Subtotal	No	Radiotherapy, dabrafenib/trametinib	Alive	27 months
#4	18 years	M	Seizure	Right temporal	Calcified, enhancing mass	Composite GG-PXA, grade 3	Gross total	Yes, new enhancement 18 months after initial operation	Reresection at 20 months and 32 months after initial operation	Alive	30 months
#5	13 years	F	Headaches	Corpus callosum	Well-circumscribed, enhancing mass	Composite GG-PXA, grade 2	Gross total	No	None (surveillance only)	Alive	29 months

EOR, extent of resection; VS, vital status.

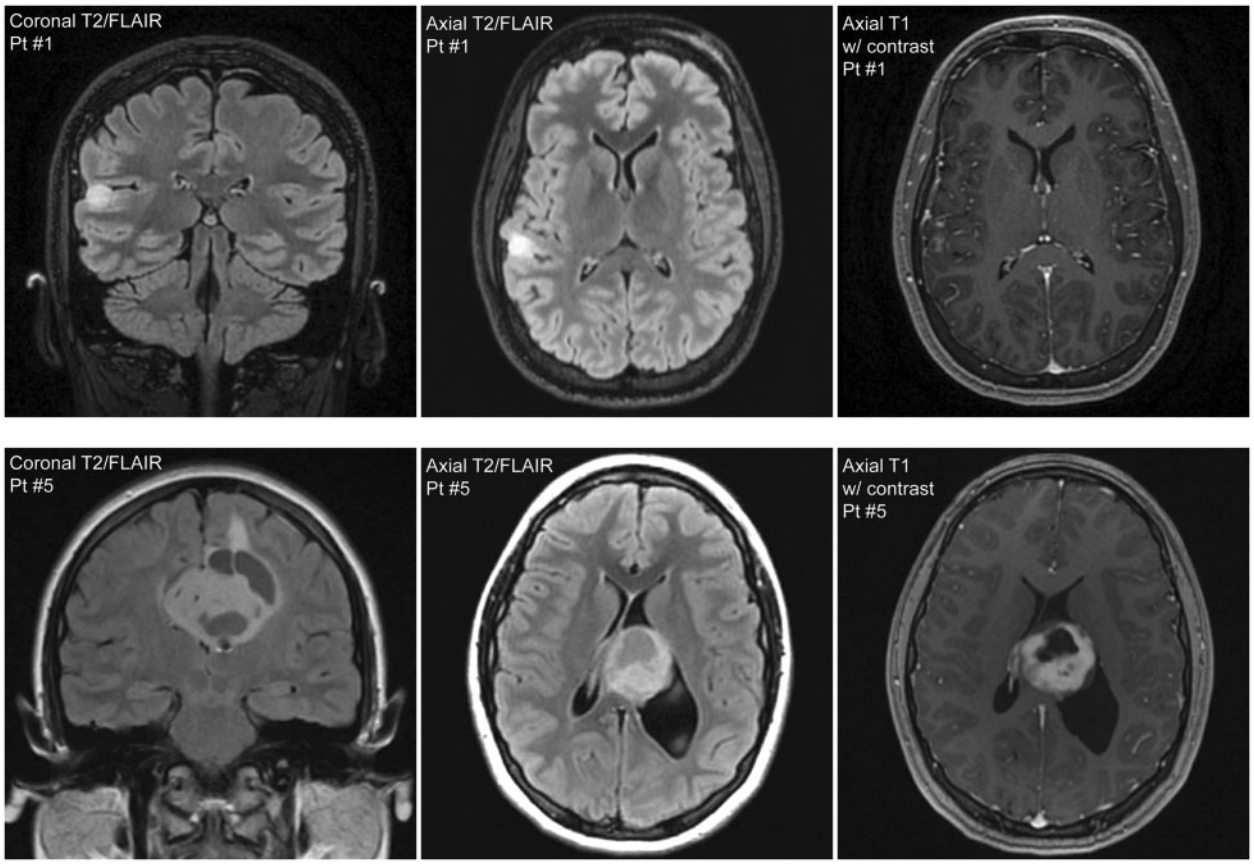

FIGURE 1. Composite pleomorphic xanthoastrocytoma-ganglioglioma may present as a solid or mixed solid/cystic mass on preoperative imaging. Magnetic resonance imaging of patient #1 showed a solitary 1.2 cm T2-hyperintense heterogeneously enhancing mass within the right superior temporal gyrus involving the posterior sylvian fissure (top row). In contrast, magnetic resonance imaging of patient #5 demonstrated a solitary 4.5 cm T2-hyperintense enhancing solid and cystic mass centered within the corpus callosum body and extending into the paramedian left frontal lobe (bottom row).

Histologic and Immunohistochemical Features of Composite PXA-GG

All 5 tumors demonstrated 2 morphologically distinct but geographically juxtaposed solid components (Fig. 2 and Supplementary Data Fig. S1). The GG component of all tumors was composed of variably sized dysmorphic ganglion cells admixed with round to mildly irregular glial cells embedded within a delicate fibrillar background. Mitotic activity was uniformly low across all 5 GG components. In contrast, the PXA component was invariably more cellular, composed of large pleomorphic glial cells within a fibrillar to desmoplastic background. Multinucleated tumor cells, vacuolated (lipidized) forms, and dysmorphic ganglion cells were variably present across the PXA components. Two PXA components (tumors #3 and #4) additionally demonstrated frequent mitotic figures (>5 mitoses per 2 mm^2) along with areas of necrosis, qualifying for CNS WHO grade 3; the remaining 3 PXA components were considered CNS WHO grade 2. Eosinophilic granular bodies and Rosenthal fibers were a common feature across both GG and PXA components. Immunohistochemistry for BRAF V600E mutant protein was positive in all assessed GG (#1, #2, #4) and PXA (#1, #2, #3, #4) components (Table 2). Additionally, all assessed GG components (#1, #2, #4, #5) demonstrated extensive p16 immunoreactivity ("overexpression"), whereas all assessed PXA components (#1, #2, #4, #5) showed loss of p16 expression—p16 is the protein product encoded by *CDKN2A*.

Targeted Sequencing Reveals Divergent Evolution in Matched PXA and GG Components

Of the 5 tumors, 3 (#1, #2, and #3) had sufficient material for comparison of paired PXA and GG components. Next-generation sequencing demonstrated the identical *BRAF* p.V600E activating hotspot mutation in the PXA and GG components of all 3 cases (Fig. 3 and Table 2). The *BRAF* mutation was the solitary oncogenic mutation identified in all 6 components, with an absence of accompanying mutations involving other frequently altered genes in central nervous system tumors including *IDH1/2*, histone H3 genes, *TERT, TP53, ATRX, NF1, FGFR1/2/3, NTRK1/2/3, PIK3CA, PIK3R1, PTEN*, and *MYBL1* (Supplementary Data Tables S2 and S3). However, along with the *BRAF* p.V600E mutation, *CDKN2A* homozygous deletion was identified in and limited to the PXA components (Supplementary Data Fig. S2). Additionally, di-

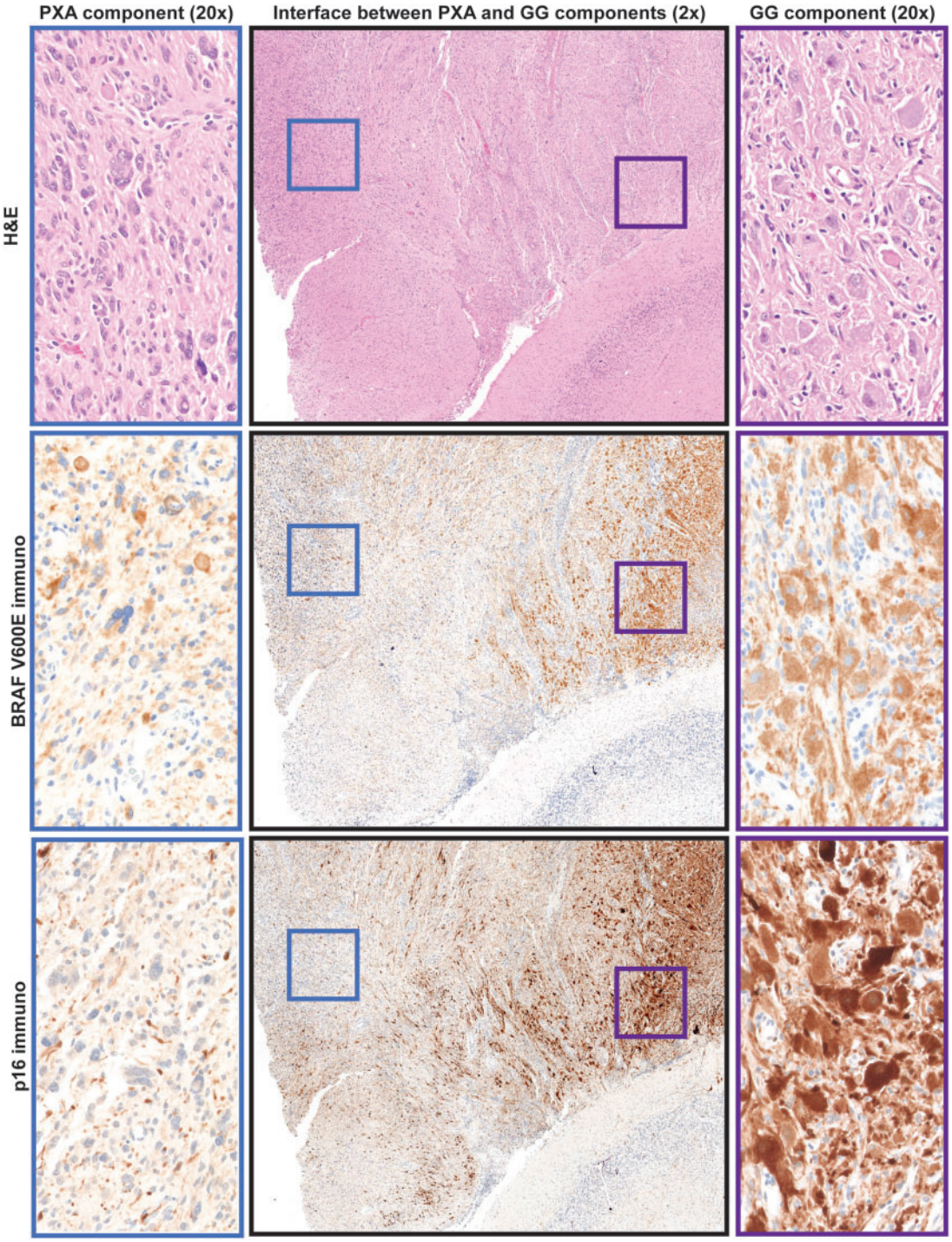

FIGURE 2. Composite pleomorphic xanthoastrocytoma-ganglioglioma are composed of 2 morphologically distinct but geographically juxtaposed solid components. Low-magnification microscopy of tumor #2 (center column) demonstrates intermingling of the 2 tumor components at the component interface. The pleomorphic xanthoastrocytoma component (left) is composed of large pleomorphic multinucleated glial cells within a fibrillar background. In contrast, the ganglioglioma component (right) is composed of variably sized dysmorphic ganglion cells admixed with round to mildly irregular glial cells. Both components demonstrate immunoreactivity for BRAF V600E mutant protein (center row) but show differential expression of p16 (bottom row)—loss of expression in the pleomorphic xanthoastrocytoma component and overexpression in the ganglioglioma component, suggestive of a related origin but divergent evolution of the 2 components.

TABLE 2. Immunohistochemical and Molecular Studies Performed in the 5 Cases of "Composite Pleomorphic Xanthoastrocytoma-Ganglioglioma"

	Immunohistochemistry Results				Next-Generation Sequencing Results				
	GG Component		PXA Component		GG Component			PXA Component	
ID	BRAF V600E Mutant Protein	p16	BRAF V600E Mutant Protein	p16	Single-Nucleotide Variants	Focal Homozygous Deletions	Other Copy Number Changes	Single-Nucleotide Variants	Focal Homozygous Deletions	Other Copy Number Changes
#1	Positive	Extensive positivity	Positive	Loss of expression	*BRAF* p.V600E	None	+7, −19p	*BRAF* p.V600E	*CDKN2A/B*	−9
#2	Positive	Extensive positivity	Positive	Loss of expression	*BRAF* p.V600E	None	None	*BRAF* p.V600E	*CDKN2A/B*	−10, −17p
#3			Positive		*BRAF* p.V600E	None	Numerous, including +7, +12, +20	*BRAF* p.V600E	*CDKN2A/B*	Numerous, including +7, +12, +20
#4	Positive	Extensive positivity	Positive	Loss of expression				*BRAF* p.V600E + *TERT* c.−124C>T	*CDKN2A/B*	Numerous
#5		Extensive positivity		Loss of expression						

GG, ganglioglioma; PXA, pleomorphic xanthoastrocytoma.

vergent copy number alterations were identified when comparing the matched PXA and GG components. Notably, in tumor #3, a subset of shared copy number alterations between the PXA and GG components was seen, including gains of whole chromosomes 7, 12, and 20. The PXA component of tumor #4 was also sequenced (without the paired GG component for comparison) and demonstrated *BRAF* p.V600E activating hotspot mutation, *TERT* c.−124C>T promoter hotspot mutation, and several copy number alterations including focal *CDKN2A* homozygous deletion on chromosome 9p21, a profile consistent with what has been reported previously in de novo high-grade PXA. Although the GG component of tumor #4 was not sequenced, the component demonstrated immunoreactivity for BRAF V600E mutant protein antibody and retained expression of p16, as noted above, whereas the PXA component demonstrated loss of p16 expression, consistent with the *CDKN2A* homozygous deletion identified on next-generation sequencing.

DISCUSSION

Here, we identify shared *BRAF* hotspot mutations between both components of PXA-GG, and *CDKN2A* homozygous deletion exclusive to the PXA component in our series of composite PXA-GG. The loss of p16 expression in PXA harboring *CDKN2A* homozygous deletion can help to differentiate this divergent component from GG with overexpression of p16 in the setting of intact *CDKN2A* alleles. Copy number alterations were relatively limited in GG components compared to PXA components, and extensive chromosomal losses were limited to CNS WHO grade 3 PXA components. These mutation and copy number findings closely recapitulate the molecular signatures of conventional PXA and GG arising in isolation (14–18). Of note, one prior study demonstrated identical *BRAF* p.V600E hotspot mutations in matched PXA and GG components in 3 composite PXA-GG, but additional copy number analysis and assessment of p16 expression or *CDKN2A* status were not performed at the time (11). Interestingly, while *BRAF*-wildtype GG and PXA are recognized (21, 22), only rare cases of confirmed *BRAF*-wildtype composite PXA-GG have been reported to date (13). Additionally, we demonstrate shared chromosomal copy number alterations between paired PXA and GG components. It is likely that these shared alterations were acquired early in tumorigenesis, implying that the PXA and GG components arose from a common origin.

These findings support divergent evolution of the PXA and GG components from a common *BRAF* p.V600E-mutant precursor lesion, with additional acquisition of *CDKN2A* homozygous deletion in the PXA component as is typically seen in conventional PXA. Conventional GG is not currently recognized to progress to PXA, although composite PXA-GG may reflect a specific point in time of tumor progression or evolution. As such, it is an intriguing possibility that some PXAs may represent tumors that transformed from an earlier GG precursor due to homozygous *CDKN2A* deletion causing this unusual form of progression. Nevertheless, additional comprehensive molecular studies

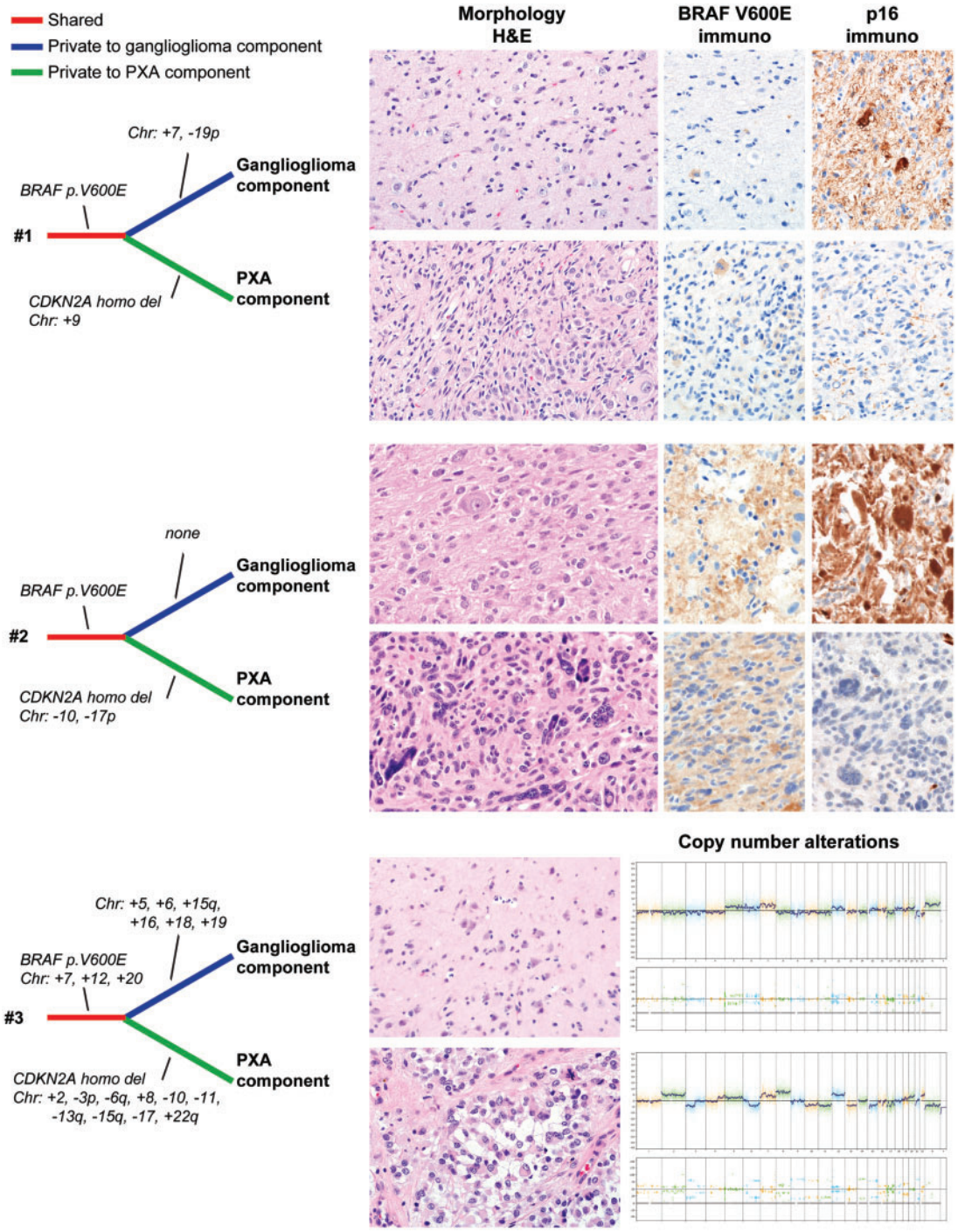

FIGURE 3. Histologically distinct components of composite pleomorphic xanthoastrocytoma-ganglioglioma demonstrate divergent molecular evolution from a common BRAF-mutant precursor lesion. Next-generation sequencing performed in cases #1, #2, and #3 demonstrated divergent copy number alterations in matched pleomorphic xanthoastrocytoma (PXA) and ganglioglioma (GG) components of each PXA-GG (left). In tumor #3, shared copy number alterations between the PXA and GG components included gain of whole chromosomes 7, 12, and 20 (bottom). Notably, the identical *BRAF* p.V600E activating hotspot mutation was identified in the PXA and GG components of all 3 cases. Immunohistochemistry for BRAF V600E mutant protein was positive in all assessed components (right). In addition to divergent copy number alterations at the whole chromosome level, *CDKN2A* homozygous deletion was limited to the PXA components. Immunohistochemistry for p16 demonstrated overexpression in the GG components and loss of expression (positivity only in rare nonneoplastic cells) in the PXA components (right).

are required to elucidate the precise relationship of composite PXA-GG to conventional PXA and GG.

ACKNOWLEDGMENTS

We thank the staff of the UCSF Clinical Cancer Genomics Laboratory for assistance with genetic profiling.

DATA AVAILABILITY

Single-nucleotide variant and copy number data are available in the electronic supplementary material. Raw sequencing data files are available from the authors upon reasonable request.

REFERENCES

1. Furuta A, Takahashi H, Ikuta F, et al. Temporal lobe tumor demonstrating ganglioglioma and pleomorphic xanthoastrocytoma components. Case report. J Neurosurg 1992;77:143–7
2. Lindboe CF, Cappelen J, Kepes JJ. Pleomorphic xanthoastrocytoma as a component of a cerebellar ganglioglioma: Case report. Neurosurgery 1992;31:353–5
3. Kordek R, Biernat W, Alwasiak J, et al. Pleomorphic xanthoastrocytoma and desmoplastic infantile ganglioglioma—have these neoplasms a common origin? Folia Neuropathol 1994;32:237–9
4. Rao C, Abdu A, Deloso D, et al. Co-occurrence of ganglioglioma and pleomorphic xanthoastrocytoma in the temporal lobe. J Neurooncol 1995;24:125–40
5. Powell SZ, Yachnis AT, Rorke LB, et al. Divergent differentiation in pleomorphic xanthoastrocytoma. Evidence for a neuronal element and possible relationship to ganglion cell tumors. Am J Surg Pathol 1996;20:80–5
6. Perry A, Giannini C, Scheithauer BW, et al. Composite pleomorphic xanthoastrocytoma and ganglioglioma: Report of four cases and review of the literature. Am J Surg Pathol 1997;21:763–71
7. Hessler RB, Kfoury H, Al-Watban J, et al. Angiomatous pleomorphic xanthoastrocytoma as a component of ganglioglioma. Ann Saudi Med 1999;19:48–51
8. Evans AJ, Fayaz I, Cusimano MD, et al. Combined pleomorphic xanthoastrocytoma-ganglioglioma of the cerebellum. Arch Pathol Lab Med 2000;124:1707–9
9. Yeh DJ, Hessler RB, Stevens EA, et al. Composite pleomorphic xanthoastrocytoma-ganglioglioma presenting as a suprasellar mass: Case report. Neurosurgery 2003;52:1465–9
10. Sugita Y, Irie K, Ohshima K, et al. Pleomorphic xanthoastrocytoma as a component of a temporal lobe cystic ganglioglioma: A case report. Brain Tumor Pathol 2009;26:31–6
11. Aisner DL, Newell KL, Pollack AG, et al. Composite pleomorphic xanthoastrocytoma-epithelioid glioneuronal tumor with BRAF V600E mutation—report of three cases. Clin Neuropathol 2014;33:112–21
12. Cicuendez M, Martinez-Saez E, Martinez-Ricarte F, et al. Combined pleomorphic xanthoastrocytoma-ganglioglioma with BRAF V600E mutation: Case report. J Neurosurg Pediatr 2016;18:53–7
13. Rosselló A, Plans G, Vidal-Sarró N, et al. Ganglioglioma progression to combined anaplastic ganglioglioma and anaplastic pleomorphic xanthoastrocytoma. Case report and literature review. World Neurosurg 2017;108:996.e17–25
14. Pekmezci M, Villanueva-Meyer JE, Goode B, et al. The genetic landscape of ganglioglioma. Acta Neuropathol Commun 2018;6:47
15. Vaubel RA, Caron AA, Yamada S, et al. Recurrent copy number alterations in low-grade and anaplastic pleomorphic xanthoastrocytoma with and without BRAF V600E mutation. Brain Pathol 2018;28:172–82
16. Phillips JJ, Gong H, Chen K, et al. The genetic landscape of anaplastic pleomorphic xanthoastrocytoma. Brain Pathol 2019;29:85–96
17. Ryall S, Tabori U, Hawkins C. Pediatric low-grade glioma in the era of molecular diagnostics. Acta Neuropathol Commun 2020;8:30
18. Vaubel R, Zschernack V, Tran QT, et al. Biology and grading of pleomorphic xanthoastrocytoma-what have we learned about it? Brain Pathol 2021;31:20–32
19. Kline CN, Joseph NM, Grenert JP, et al. Targeted next-generation sequencing of pediatric neuro-oncology patients improves diagnosis, identifies pathogenic germline mutations, and directs targeted therapy. Neuro Oncol 2017;19:699–709
20. Lucas CG, Gupta R, Doo P, et al. Comprehensive analysis of diverse low-grade neuroepithelial tumors with FGFR1 alterations reveals a distinct molecular signature of rosette-forming glioneuronal tumor. Acta Neuropathol Commun 2020;8:151
21. Phillips JJ, Gong H, Chen K, et al. Activating NRF1-BRAF and ATG7-RAF1 fusions in anaplastic pleomorphic xanthoastrocytoma without BRAF p.V600E mutation. Acta Neuropathol 2016;132:757–60
22. Lucas CG, Abdullaev Z, Bruggers CS, et al. Activating NTRK2 and ALK receptor tyrosine kinase fusions extend the molecular spectrum of pleomorphic xanthoastrocytomas of early childhood: A diagnostic overlap with infant-type hemispheric glioma. Acta Neuropathol 2022;143:283–6